Deconstructing isolation-by-distance: the genomic consequences of limited dispersal

Stepfanie M. Aguillon*[,1,2], John W. Fitzpatrick[1,2], Reed Bowman[3], Stephan J. Schoech[4], Andrew G. Clark[1,5], Graham Coop[6,7], Nancy Chen[2,6,7]

[1] Department of Ecology and Evolutionary Biology, Cornell University, Ithaca, New York 14853, USA

[2] Cornell Laboratory of Ornithology, Cornell University, 159 Sapsucker Woods Road, Ithaca, New York 14850, USA

[3] Archbold Biological Station, 123 Main Dr., Venus, Florida 33960, USA

[4] Department of Biological Sciences, University of Memphis, Memphis, Tennessee 38152, USA

[5] Department of Molecular Biology and Genetics, Cornell University, Ithaca, New York 14853, USA

[6] Center for Population Biology & Department of Evolution and Ecology, University of California, Davis, Davis, CA 95616, USA

[7] Co-senior author

* Corresponding author: sma256@cornell.edu

Abstract

Geographically limited dispersal can shape genetic population structure and result in a correlation between genetic and geographic distance, commonly called isolation-by-distance. Despite the prevalence of isolation-by-distance in nature, to date few studies have empirically demonstrated the processes by which it is generated within a pedigreed and genotyped population. Intensive, long-term demographic studies and exhaustive genomic surveys in the Florida Scrub-Jay (*Aphelocoma coerulescens*) provide an excellent opportunity to investigate the influence of dispersal on genetic structure. Here, we use a panel of genome-wide SNPs and extensive pedigree

information to explore the role of limited dispersal in shaping patterns of isolation-by-distance in both sexes, and at an exceedingly fine spatial scale (within ~10 km). Isolation-by-distance patterns were stronger in male-male and male-female comparisons than in female-female comparisons, consistent with observed differences in dispersal propensity between the sexes. Using the pedigree, we demonstrated how various genealogical relationships contribute to fine-scale isolation-by-distance. Simulations using field-observed distributions of male and female natal dispersal distances showed good agreement with the distribution of geographic distances between breeding individuals of different pedigree relationship classes. Furthermore, we can accurately reconstruct observed isolation-by-distance patterns in autosomal and Z-linked SNPs using coalescent simulations parameterized by the observed dispersal curve, population density, and immigration rate. Therefore, patterns of fine-scale isolation-by-distance can be well understood as a result of limited dispersal over contemporary timescales in the Florida Scrub-Jay.

Introduction

The movement of individuals over the landscape (dispersal) influences biological processes and diversity at many levels [1], ranging from interactions between individuals to persistence of populations or species over time [2-4]. Limited dispersal is also central to generating and maintaining spatial genetic structure within species. In particular, geographically-limited dispersal can result in isolation-by-distance, a pattern of increased genetic differentiation [5, 6] or, conversely, decreased genetic relatedness [7-9] between individuals as geographic distance increases. This pattern results because genetic drift can act to differentiate allele frequencies faster than dispersal can homogenize them among geographically distant populations. A correlation between genetic differentiation and geographic distance is observed in many empirical systems, consistent with isolation-by-distance being a dominant process in structuring genetic diversity [10, 11].

Despite the fact that correlations between genetic differentiation and geographic distance are common across many types of organisms, to date, few empirical demonstrations exist for how contemporary patterns of dispersal contribute to the observed pattern of isolation-by-distance. This is, in part, because dispersal is hard to estimate empirically, as it requires monitoring many individuals over long periods of time across the full range of potential dispersal distances [12]. In addition, the effective population density of reproducing individuals must be known in order to parameterize genetic drift in models of isolation-by-distance. Therefore, in practice it is hard to know whether the observation of isolation-by-distance is truly consistent with contemporary patterns of dispersal. Indeed, many studies use genetic isolation-by-distance patterns to

infer dispersal distances, as a substitute for the more difficult exercise of measuring dispersal directly in the field [13-17]. A second issue is that in most studied systems, populations are compared over large spatial scales, so the pattern of isolation-by-distance reflects the dynamics of genetic drift and dispersal over tens of thousands of generations. These empirical patterns reflect large-scale population movements (*e.g.*, expansions from glacial refugia [18]) that may not reflect the equilibrium outcome of individual dispersal and genetic drift. While studies have reported fine-scale population structure [19-25], it has been difficult to deconstruct these patterns to understand what mechanisms actually create them.

Patterns of isolation-by-distance can reflect underlying biological processes. Since the early development of the isolation-by-distance theory, differences in mating systems and dispersal propensity have both been known to generate differences in isolation-by-distance patterns [5]. In many organisms, dispersal often differs between the sexes: males disperse farther in mammals (male-biased dispersal), but females disperse farther in birds (female-biased dispersal) [26, 27]. When dispersal patterns differ between the sexes, the less dispersive sex tends to have stronger overall genetic structure than the more dispersive sex [21, 28, 29]. Similarly, sex-biased dispersal is expected to result in different levels of genetic structure in markers with different inheritance patterns. For example, in systems where females are more dispersive, autosomes may exhibit higher genetic differentiation than maternally inherited markers (*e.g.* mitochondrial DNA), but lower genetic differentiation than the Z chromosome (females are homogametic in ZW systems) [16, 30, 31].

Here we examine the causes of fine-scale isolation-by-distance in a non-migratory bird, the Florida Scrub-Jay (*Aphelocoma coerulescens*), based on a long-term population study that yields high-quality genetic and pedigree information for many individuals as well as particularly detailed information on individual dispersal distances. Florida Scrub-Jays have limited, female-biased natal dispersal, and individuals essentially never move once established as a breeding adult [32, 33]. A population of Florida Scrub-Jays at Archbold Biological Station in central Florida has been the focus of intense monitoring since 1969, resulting in observed natal dispersal distances for hundreds of individuals and an extensive pedigree [32, 34, 35]. Moreover, nearly all nestlings and breeders present in the population during the past two decades were genotyped in a recent study [36]. These long-term dispersal, pedigree, and genomic data make the Florida Scrub-Jay an unusually tractable study system in which to explore how dispersal influences patterns of isolation-by-distance.

Previous work on Florida Scrub-Jays using microsatellite markers has shown isolation-by-distance across multiple populations [3]. Here, we present evidence for fine-scale isolation-by-distance within a single contiguous population of Florida Scrub-Jays, and combine genetic, pedigree, and dispersal information to reveal how patterns of isolation-by-distance are created in nature. We find more isolation-by-distance in males than in females, corresponding to predicted differences resulting from female-biased dispersal patterns. We break down our data into pedigree relationships to demonstrate how isolation-by-distance is a consequence of close relatives living geographically close together. We perform simulations that can reconstruct the empirical distances between individuals of different kinship classes using only the dispersal curves. Finally, we use

110 coalescent simulations parameterized by the dispersal curve, population density, and immigration rate to yield an excellent fit to observed isolation-by-distance patterns.

112

Results/Discussion

114 *Limited dispersal results in isolation-by-distance at small spatial scales*

We documented natal dispersal distances for 382 male and 290 female Florida 116 Scrub-Jays that were born and established as breeders within the population at Archbold Biological Station between 1990-2013. Dispersal curves for both males and 118 females were strongly leptokurtic, consistent with previous studies (Fig 1A; [3, 34]). Here we considered only dispersal within the Archbold population; therefore, our 120 dispersal curves do not capture any long-distance dispersal events, which rarely occur [3]. Females disperse significantly farther than males, with a median ± SE distance of 122 1,149 ± 108 m and 488 ± 43 m, respectively (Wilcoxon rank sum test, $p = 2.2 \times 10^{-16}$). The extremely short male dispersal distances compared to females may be due in part 124 to differences in territory acquisition between the sexes. Florida Scrub-Jay males are able to acquire breeding territories through budding from the parental territory or 126 inheritance of the parental territory [32], while territory budding and inheritance is extremely rare in females [34].

128 To explore the genetic implications of this limited, sex-biased dispersal, we genotyped all breeding adults in the Archbold population in 2003, 2008, and 2013 (n = 130 513) at 7,843 autosomal SNPs and 277 Z-linked SNPs [36]. We conducted principal component analysis (PCA) separately for all breeding adults, male breeders, and 132 female breeders to visually summarize patterns of autosomal genetic variation within

our population. We see genetic differentiation along the north/south axis of Archbold in the first two PC axes when we map breeders to their breeding territories (Fig 1B, S1). Indeed, the top two principal components (PC1 and PC2, 14.6% and 13.1% of the variation, respectively) are significantly correlated with north-south position under the Universal Transverse Mercator coordinate system (henceforth “UTM northing”; Table S1). We found significant correlations with UTM northing for both PC1 and PC2 in males, but only PC1 is significantly correlated with UTM northing in females (Fig S2; Table S1). Correlation coefficients for PC1 with UTM northing are higher in males than in females (Table S1). This fine-scale spatial structure is likely a direct result of the unusually limited natal dispersal and female-biased dispersal of these birds (Fig 1A; overall median ± SE = 647 ± 57 m).

To test for isolation-by-distance, we quantified autosomal genetic relatedness between all possible pairs of individuals in the dataset as the estimated proportion of the genome shared identical-by-descent (IBD). Under a model of isolation-by-distance, IBD should decrease as the distance between individuals in a pair increases. Plotting genetic relatedness against geographic distance for all unique pairs across all years, we found a clear pattern of isolation-by-distance (Fig 1C) at a fine spatial scale (Archbold is ~10 km from north to south; Fig 1B). We used Mantel correlograms to compare pairwise geographic and genetic distances (IBD) across all pairwise comparisons, all male-male pairs, and all female-female pairs. We find significant correlations at more distance classes in all breeders and male-male pairs than in female-female pairs (Table S2).

To measure the strength of isolation-by-distance in different subsets of the data, we fitted loess curves and used them to estimate the distance (δ) where the IBD drops

156 halfway to the mean from its maximum value. A lower δ indicates a more rapid decay of genetic relatedness by geographic distance, *i.e.*, more isolation-by-distance. We
158 bootstrapped pairs of individuals to obtain 95% confidence intervals (CI) to assess significance and found stronger isolation-by-distance patterns in male-male (δ = 620 m,
160 95% CI = [604, 631]) and male-female comparisons (δ = 645 m, [622, 665]) than in female-female comparisons (δ = 903 m, [741, 1261]; Fig 1C), which is consistent with
162 the strongly female-biased dispersal observed in this system.

Because of the detailed pedigree information available for the Florida Scrub-Jay
164 population within Archbold, we have a rare opportunity to decompose the isolation-by-distance patterns found in this population by familial relationship. The Florida Scrub-Jay
166 pedigree from our study population consists of 12,738 unique individuals over 14 generations and is largely complete (see Table S3 for a summary of the pedigree); here
168 we identify relationships up to fourth cousins. For each pair of individuals in our dataset, we extracted their closest pedigree relationship in the population pedigree (*e.g.*, 1,532
170 of 130,618 pairs have a relationship closer than first cousins; Table S3) and calculated the pedigree-based coefficient of relationship (*r*). We plotted IBD for pairs of individuals
172 against the geographic distance between those individuals, coloring points by their pedigree relationship (Fig 2). This clearly illustrated how isolation-by-distance results, in
174 part, from closely related individuals, such as parent-offspring and full-siblings, remaining physically close together as breeders within neighborhoods of contiguous
176 territories (Fig 2). The stronger signal of isolation-by-distance in male-male comparisons (Fig 2A) seems to be driven by the particularly short geographic distances between
178 individuals in the highest pedigree relatedness classes (*e.g.*, parent-offspring, full-

siblings, grandparent-grandchild, half-siblings, and aunt/uncle-nibling ["nibling" is a gender-neutral term for niece and nephew]).

Another way of visualizing how dispersal generates a pattern of isolation-by-distance is to plot the distribution of geographic distances separating pairs of individuals with different pedigree relationships (Fig 3A). Close relatives tend to be located closer geographically: for example, the median geographic distance between parent-offspring pairs is significantly lower than that between full-siblings (Wilcoxon rank sum test, $p = 5.20 \times 10^{-9}$), and the distance between full-siblings is significantly lower than the distance between pairs with $r = 0.25$ (half-siblings, grandparent-grandchildren, and aunt/uncle-niblings; Wilcoxon rank sum test, $p = 0.01$). More generally, if we compare a given pedigree relationship class (r) with the pedigree relationship class that is half as related ($0.5r$), we find shorter distances in the more related pairs for all sequential comparisons out to third cousins (comparing pairs with r to $0.5r$, Wilcoxon rank sum test, $p < 0.003$ for all except for the comparison between $r = 0.0625$ and $r = 0.03125$; Table S4). Geographic distances between two males with a close, known pedigree relationship are shorter than in either female-female or male-female comparisons (Fig 3A; Table S5), and this pattern holds generally in comparisons up to second cousins.

We can further assess the contribution of various relationship types by sequentially removing pedigree relationship classes and observing the resulting isolation-by-distance curves (Fig 3B). As expected, the relationship between IBD and geographic distance flattens and the strength of isolation-by-distance (measured by δ) decreases as closely related pairs are removed (Fig 3B, Table S6). For example, removing pairs with $r > 0.5$ (parent-offspring and full-siblings) and $r > 0.25$ (parent-

offspring, full-siblings, half-siblings, grandparents, and aunt/uncle-nibling) caused significant increases in δ (Fig 3B, Table S6). However, even after removing all pairs with $r \geq 0.0625$ we still see a significant pattern of isolation-by-distance (Table S6). Therefore, isolation-by-distance is not driven only by highly related individuals. Instead, it appears that highly related individuals ($r > 0.25$) drive the strength of the observed isolation-by-distance patterns, but isolation-by-distance still exists even when these individuals are removed from the dataset. This suggests that isolation-by-distance, even at this spatial scale, is not a result of dispersal events over only one or two generations, but instead is generated from dispersal events over many generations.

Isolation-by-distance patterns are also present in Z-linked SNPs

Patterns of genetic diversity on the Z chromosome are expected to differ from those on the autosomes because of the difference in inheritance patterns and sex-specific dispersal behavior [37]. In birds, males are the homogametic sex (ZZ), while females are heterogametic (ZW). Thus, the Z chromosome spends two-thirds of its evolutionary history in males. In addition, the Z chromosome has a smaller effective population size compared to the autosomes [38]. These facts lead to two predictions: (1) Owing to the reduced effective population size of the Z chromosome, we expect to see higher IBD on the Z compared to the autosomes. (2) Because females disperse much farther than males in this system, we expect to find more isolation-by-distance in Z-linked SNPs than in autosomal SNPs [31, 37].

We separately assessed patterns of isolation-by-distance in 277 Z-linked SNPs. PCA results for Z-linked markers are similar to those observed in autosomes. We found

significant correlations for PC1 and PC2 with UTM northing, though correlations between PC2 and UTM northing were significant only for all breeders and male only comparisons (Fig S3, Table S1). To fairly compare autosomes and Z chromosomes, which differ in the number of SNPs present, we used unbiased estimates of IBD for Z-linked and autosomal SNP comparisons (which are not bounded by 0 and 1 as are traditional estimates of IBD). Similar to autosomal SNPs, isolation-by-distance patterns in Z-linked SNPs are stronger in male-male comparisons (δ = 615 m, [592, 639]) than in either female-female (δ = 979 m, [673, 2048]) or male-female comparisons (δ = 637 m, [601, 674]; Fig S4). In accordance with theoretical predications, mean IBD is higher for the Z chromosome (0.014, [0.013,0.015]) compared to the autosomes (0.0027, [0.0024,0.0030]; Fig 4). However, we do not find evidence for more isolation-by-distance on the Z chromosome: δ for Z-linked SNPs (647 m, [620, 677]) is not significantly different than δ for autosomal SNPs (621 m, [608, 633]). It is possible that we lack the power to estimate IBD on the Z chromosome accurately, given the small number of Z-linked SNPs available (277), which leads to more noise and uncertainty in the estimates of IBD on the Z chromosome and therefore a high variance in δ. This is consistent with the larger standard errors for the Z (Fig 4) and the larger confidence interval for δ on the Z. Future work will increase marker density on the Z to increase resolution and will incorporate maternally-inherited markers like the W and mitochondria to provide additional insights into the consequences of sex-biased dispersal on markers with different inheritance modes.

Simulations can reconstruct observed geographic and genetic structure

248 To test our understanding of the population mechanisms leading to fine-scale isolation-by-distance, we used simulations to explore whether observed patterns could
250 be predicted strictly by dispersal curves and other population parameters. We first conducted simulations of local dispersal in a contiguous population to determine how
252 well the observed distribution of geographic distances between individuals of known pedigree relationships was predicted by the observed natal dispersal curves. Assuming
254 that the dispersal curves are constant and that dispersal distance has negligible heritability, we simulated the distance between individuals of a known, close pedigree
256 relationship using random draws from the sex-specific dispersal curves. For example, for female first cousins, we first simulated the dispersal distances of the parental
258 siblings from the grandparental nest (randomly picking their sexes). We then added the simulated dispersal distances of the two female cousins from their respective parental
260 nests and calculated the distance (d) between them (Fig 5A). We repeated this procedure 10,000 times to obtain a distribution of d.

262 We found that the dispersal curve simulations nicely reconstruct the observed distribution of geographic distances between related individuals up to first cousins
264 (Kolmogorov-Smirnov Test, $p > 0.05$ for most pairs). For more distantly related pairs (second cousins), the simulations are significantly different from the observed distances
266 (Kolmogorov-Smirnov Test, $p < 0.008$ for male-female and female-female pairs; Fig 6; Table S7). Notably, the observed distributions in male-male comparisons of closely
268 related individuals (full siblings and uncle-nephew) are significantly different from the simulated distributions – we see more short distances between individuals in the
270 observed data than expected (Fig 6; Table S7). Our dispersal simulations did not

recover empirical distances for distantly related pairs because we assumed a continuous population over infinite space. In nature, we know that dispersal movements are largely restricted to the bounded population within the study population. Because the natal dispersal curves include only within-population dispersal events, we do not think a violation of this assumption is problematic for simulations of closely related pairs, which involve just a few dispersal events. To accurately simulate distances between distantly related pairs, we would need to consider the spatial extent of the population and not allow dispersal movements outside of population boundaries.

Malécot envisioned IBD as being due to the chain of ancestry running from present day individuals back to their shared ancestors ("les chaînes de parenté gamétique"; Fig 5B; [9, 39]). These ideas are the forerunner of modern coalescent theory [40, 41]. Malécot's interpretation of the relationship between IBD and geographic distance reflects the fact that geographically close pairs of individuals are more likely to be closely related, *i.e.*, trace back to a more recent common ancestor (coalesce), than geographically distant individuals [9].

To empirically demonstrate the underlying mechanisms behind Malécot's model, we calculated the expected IBD values as a function of geographic distance for male-male, male-female, and female-female pairs using a spatially-explicit coalescent model. We parameterized these simulations using the observed pedigree, dispersal curves, immigration rate, and basic demographic information about the study system. For a given pair of individuals, we traced the ancestry of their two alleles, at each autosomal locus, backwards in time until the two lineages find a common ancestor or at least one of the lineages was a descendent of an immigrant into the population (Fig 5C). The

probability that a lineage in a given generation was brought into the population by an immigrant (*M*) is given by the proportion of individuals who are immigrants. If one or both of our lineages traced back to an immigrant, we assigned the pair of individuals the observed level of IBD between immigrants. We kept track of the geographic location of each non-immigrant ancestor by sampling dispersal events from the sex-specific natal dispersal curves. If our lineages are distance d_k apart in generation k, the probability of our lineages finding a shared ancestor in the next generation back (k+1) is given by the proportion of pairs that are d_k apart who are full/half siblings or parent-offspring pairs (see Fig S5). If the two lineages traced to one of these relationships, we assigned them the observed level of IBD for that relationship. We simulated expected IBD values for many pairs of individuals at a given distance bin. Our pedigree-based simulations recovered the observed pattern of isolation-by-distance for both autosomal and Z-linked loci, explaining a high proportion of the variance in mean IBD across distance for all three comparisons (coefficient of determination > 0.75; Fig 7, S6; Table S8). These results suggest that dispersal can generate isolation-by-distance over short timescales in this population.

Future directions

Here we have used single-marker estimates of genome-wide IBD to study relatedness. Additional power to infer recent demography and dispersal history can be gained by studying shared IBD blocks – linked segments of the genome that are shared IBD between pairs of individuals [42-44]. A number of methods exist for inferring IBD blocks from dense genotyping or sequencing data [45]. By tracing the spatial distribution

of IBD blocks of varying lengths, studies of short-scale IBD can uncover how recent dispersal shapes the transmission of genomic segments across geography. Also, we will extend this approach across populations within the statewide range of this species to assess how dispersal shapes patterns of genetic variation over larger spatial scales. This question has vital conservation implications, as for example, decreasing rates of immigration are driving increased inbreeding depression within the Archbold population [36].

Conclusion

Isolation-by-distance is a commonly observed pattern in nature. Despite its ubiquity and the frequent use of isolation-by-distance patterns to indirectly estimate dispersal in diverse organisms, few studies to date have deconstructed the causes of isolation-by-distance. Here, we have shown how limited dispersal can result in isolation-by-distance in the Florida Scrub-Jay. The unusually short dispersal distances in this species allows us to detect a signal of isolation-by-distance within a single, small contiguous population over just a few generations. In systems with longer dispersal distances, patterns of isolation-by-distance will likely only be observed over larger spatial scales, and reflect relatedness over potentially much longer timescales. The extensive dispersal, pedigree, and genomic data in this well-studied system provided a rare opportunity to empirically unpack Malécot's isolation-by-distance model [9]: we have shown how limited dispersal leads to closely related individuals being located closer together geographically, which results in a pattern of decreased genetic relatedness with increased geographic distance.

340

Materials and Methods

342 *Study system: the Florida Scrub-Jay*

The Florida Scrub-Jay is a cooperatively breeding bird endemic to Florida oak
344 scrub habitat [32, 33]. Individuals live in groups consisting of a breeding pair and non-breeding helpers (often previous young of the breeding pair) within territories that are
346 defended year-round. A population of Florida Scrub-Jays at Archbold Biological Station (Venus, FL) has been intensely monitored by two groups for decades: the northern half
348 by Woolfenden, Fitzpatrick, Bowman, and colleagues since 1969 [32, 34] and the southern half by Mumme, Schoech, and colleagues since 1989 [35, 46]. Standard
350 population monitoring protocols in both studies include individual banding of all adults and nestlings, mapping of territory size and location, and surveys to determine group
352 composition, breeding status/success, and individual territory affiliation [32, 34]. Immigration into our study population is easily assessed because every individual is
354 uniquely banded (so any unbanded individual is an immigrant). Blood samples for DNA have been routinely obtained from all adults and day 11 nestlings through brachial
356 venipuncture since 1999. This intense monitoring has generated a pedigree of 14 generations over 46 years. All activities have been approved by the Cornell University
358 and University of Memphis Institutional Animal Care and Use Committees and permitted by the U.S. Geological Survey, the U.S. Fish and Wildlife Service, and the Florida Fish
360 and Wildlife Conservation Commission.

Here, we measured dispersal distances of individuals banded as nestlings within
362 Archbold and that subsequently bred within Archbold between 1990 and 2013 (382

males and 290 females). We began our sampling in 1990 because the study site was expanded to its current size by 1990; hence, dispersal measures before this year are systematically shorter (*i.e.,* lack the longer distances). Thus, our most comprehensive measure of dispersal tendencies of individuals residing within Archbold spans 24 years. We measured natal dispersal distance as the distance from the center of the natal territory to the center of the first breeding territory, in meters using ArcGIS Desktop 10.4 [47], independent of the age of first breeding (definition from [48]).

As part of a previous study, 3,984 individuals have been genotyped at 15,416 genome-wide SNPs using Illumina iSelect Beadchips [36]. Details of SNP discovery, genotyping, and quality control can be found in [36]. Here, we focused on breeding adults in Archbold during the years 2003, 2008, and 2013 (n = 513), when almost all individuals present have been genotyped. Autosomal SNPs were pruned for linkage disequilibrium using PLINK v1.07 [49]. Our final dataset included 7,843 autosomal and 277 non-pseudoautosomal Z-linked SNPs. All of the presented analyses were conducted on the combined dataset across all three years. For any individuals present in multiple years, we randomly selected presence in a single year for inclusion in this combined analysis.

Relatedness measures

To determine genetic relatedness, we estimated the proportion of the genome shared IBD relative to the population frequency for all individual pairwise comparisons within and across years using the 'genome' option in PLINK v1.07 [49] for autosomal SNPs and a custom R script for Z-linked SNPs (S1 File). IBD for Z-linked SNPs was

386 calculated using a method of moments approach using observed allele counts similar to that in [49]. IBD values reported by PLINK are constrained to biologically plausible
388 values in a final transformation step. To avoid introducing biases when comparing IBD estimates obtained from very different numbers of SNPs (on the Z chromosome versus
390 the autosomes), we used untransformed autosomal and Z-linked IBD values for comparisons between the autosomes and Z. All IBD calculations used allele
392 frequencies from the sample of all individuals in the population through time. See S1 Text for further details and S1 File for the R code.

394 Additionally, we estimated relatedness of all individual pairwise comparisons using the pedigree. We calculated the coefficient of relationship by using the 'kinship'
396 function within the package kinship2 [50] in R v3.2.2 [51] and multiplied the values by two (to convert them from kinship coefficients). The pedigree-based coefficient of
398 relationship was calculated separately for expectations under autosomal and Z-linked scenarios using the 'chrtype' option within the 'kinship' function. Because kinship2
400 assumes an XY system, we swapped the sex labels of our individuals and swapped mothers and fathers in the pedigree to accurately calculate the coefficient of relationship
402 for a ZW system. The autosomal coefficient of relationship r and IBD are highly correlated (Fig S7; linear regression: $t = 688.8$, $p < 0.0001$, $R^2 = 0.7841$). Because
404 genomic estimators of relatedness are more precise than pedigree-based estimators [52], we only report results for genomic measures of relatedness (see Fig S8, S9 and
406 Table S2 for analyses using pedigree-based measures of relatedness).

408 *Isolation-by-distance in genetic and pedigree data*

We used three approaches to statistically test for isolation-by-distance patterns in our data. First, we conducted principal component analysis on the autosomal and Z-linked IBD data using custom Perl and R scripts. We conducted separate analyses on males only, females only, and all individuals. We then compared the first two PC axes from each analysis with the UTM northing values of the territory centroids for each individual using Spearman rank correlations.

Second, we conducted Mantel correlogram tests using the 'mantel.correlog' function in the vegan package [53] in R v3.2.2 [51]. Mantel tests compare two distance matrices and test for significance through permutation of the matrix elements [54, 55]. Here, we used Mantel tests to compare a matrix of individual pairwise comparisons of geographic distances to a matrix of pairwise comparisons of relatedness between individuals (either estimated from the genomic data or from the pedigree, and for autosomes or the Z chromosome). We conducted separate analyses for comparisons between males only, females only, and all individuals. Note that we cannot conduct Mantel correlograms on male-female comparisons alone, as we cannot use unbalanced matrices in this type of analysis. We limited our analyses to the following distance class bins to ensure that enough comparisons fell within each bin: 250-750 m, 750-1250 m, 1250-1750 m, 1750-2250 m, 2250-2750 m, 2750-3250 m, 3250-3750 m, 3750-4250 m, 4250-4750 m, 4750-5250 m. We did not include comparisons between breeders in the same territory or self-self comparisons (distance = 0). We performed 10,000 permutations to obtain corrected *p*-values.

Finally, we fitted a loess curve to the scatterplot of IBD and geographic distance between pairs of individuals. We tested for isolation-by-distance by determining whether

IBD at the smallest distance interval was larger than the overall mean. To measure the strength of isolation-by-distance, we estimated the distance, which we define as δ, where IBD drops halfway to the mean from its maximum value. To assess uncertainty in these estimates, we used a bootstrapping method in which we randomly resampled pairs with replacement, fitted a loess curve, and estimated IBD at distance bin 0, mean IBD, and δ. We repeated this procedure 1,000 times to obtain 95% bias-corrected and accelerated bootstrap confidence intervals.

Dispersal simulations

We used simulations to determine whether we could generate the observed distribution of geographic distances between related pairs using only the natal dispersal curve. For each of several focal pairwise relationships (full-siblings, aunt/uncle-nibling, first cousins, and second cousins), we simulated dispersal events starting at their common ancestral nest and then recorded the resulting distance between the two focal individuals using a custom script in R (Fig 5A; S2 File). We located the shared ancestral nest of the birds at (0,0) in an unbounded two-dimensional habitat. The number of dispersal events for a given focal pair ranged from two (full-siblings) to six (second cousins). Dispersal distances were randomly sampled from the known dispersal curves for males and females (Fig 1A). The sexes of the final individuals in the focal pair were fixed (either male-male, male-female, or female-female), and we randomly sampled the sexes of ancestral individuals up to the common ancestral nest using a coin flip. For each dispersal event, we randomly sampled a dispersal angle (from 0-360°) and a dispersal distance from the sex-specific dispersal distribution. We performed this

simulation 10,000 times for each focal pairwise relationship, calculating the resulting distance between the two focal individuals each time. We determined the empirical distances between individuals of different pedigree relationships and compared the observed distributions to the simulated distributions using Kolmogorov-Smirnov tests. Code for the dispersal simulations is included in S2 File.

Coalescent simulations

We generated the expected isolation-by-distance pattern for the autosomes and the Z chromosome given the observed dispersal curves and immigration rate using spatially-explicit pedigree-based simulations inspired by Malécot's model of isolation-by-distance [9]. For each pair of individuals, we simulated their lineages backwards in time until we reached a common ancestor or one or more of the lineages was a descendent of an immigrant into the population (Fig 5C). In each generation g, we first sampled a dispersal distance from the empirical sex-specific dispersal curve (Fig 1A) and a dispersal angle uniformly at random and calculated the geographic distance d_g between the two individuals. After the first dispersal event, we randomly assigned sex for all ancestors. We then calculated the probability that the two lineages located at distances (d_1, …, d_g) did not coalesce (share a common ancestor) or have an immigrant ancestor in the previous $g - 1$ generations and the probability that they either coalesce or have an immigrant ancestor in generation g. Given the relatively small population size and high immigration rate, we found that nearly all pairs either shared a common ancestor or had an immigrant ancestor within 10 generations, and so we used $g \leq 10$ (increasing this limit had no effect on our results). Here we define the probability that two individuals

478 share a common ancestor in the preceding generation as the probability the pair is closely related (parent-offspring, full-siblings, or half-siblings). For a pair of individuals at
480 distance *d*, we estimated the probability they are parent-offspring ($P_p(d)$), full-siblings ($P_f(d)$), or half-siblings ($P_h(d)$) from the observed pedigree and distances between these
482 relative classes (Fig S5). We calculated the sex-specific probability an individual is an immigrant as the proportion of breeding male or female individuals in a given year who
484 were not born in Archbold (M = 0.197 for males and 0.345 for females). Using mean IBD values for immigrant-immigrant and immigrant-resident pairs obtained from our data, we
486 estimated the expected proportion of the genome shared IBD for a given pair of individuals as follows:

$$\hat{Z} = \sum_{g=1}^{10}\left[\prod_{k=1}^{g-1}(1-M)^2[1-P_p(d_k)-P_f(d_k)-P_h(d_k)]\right]\times\left[P_p(d_g)\mathbb{E}(Z_p)+P_f(d_g)\mathbb{E}(Z_f)\right.$$

$$\left.+P_h(d_g)\mathbb{E}(Z_h)+2M(1-M)\mathbb{E}(Z_r)+M^2\mathbb{E}(Z_m)\right]$$

488 Where E(Z_p), E(Z_f), and E(Z_h) are the expected IBD values for parent-offspring, full-sibling, and half-sibling pairs, respectively (Table S9). E(Z_m), and E(Z_r) are the sex-
490 specific empirical mean IBD values for immigrant-immigrant and immigrant-resident pairs, respectively. Because we found a pattern of isolation-by-distance in immigrant-
492 immigrant pairs, we used expected IBD values for immigrant-immigrant and immigrant-resident pairs conditional on distance. We binned distances into 15 quantiles and ran
494 1,000 simulations for each distance bin. To evaluate the fit of our model, we calculated the coefficient of determination R^2 for each type of comparison as follows:

$$R^2 = 1 - \frac{\sum_i\left(y_i-\hat{Z}_i\right)^2}{\sum_i(y_i-\bar{y}_i)^2}$$

Where y_i is the mean observed IBD value in distance bin i and Z_i is the mean simulated IBD value in distance bin i. See S2 Text for the full derivation of our model and S3 File for the R code.

Acknowledgments

We thank the many students, interns, and staff at Archbold Biological Station and the University of Memphis who collected the dispersal data. We thank the members of the Harrison, Clark, Lovette, and Coop labs for thoughtful comments on this manuscript. In memory of Richard G. Harrison without whom this collaboration would not have been formed.

REFERENCES

1. Clobert J, Danchin E, Dhont AA, Nichols JD. Dispersal. Oxford, UK: Oxford University Press; 2001.
2. Coulon A, Fitzpatrick JW, Bowman R, Lovette IJ. Mind the gap: genetic distance increases with habitat gap size in Florida scrub jays. Biol Lett. 2012;8(4):582-5. doi: 10.1098/rsbl.2011.1244. PMID: 22357936.
3. Coulon A, Fitzpatrick JW, Bowman R, Lovette IJ. Effects of habitat fragmentation on effective dispersal of Florida scrub-jays. Conserv Biol. 2010;24(4):1080-8. doi: 10.1111/j.1523-1739.2009.01438.x. PMID: 20151985.
4. Duckworth RA, Badyaev AV. Coupling of dispersal and aggression facilitates the rapid range expansion of a passerine bird. Proc Natl Acad Sci USA. 2007;104(38):15017-22. doi: 10.1073/pnas.0706174104. PMID: 17827278.
5. Wright S. Isolation by distance under diverse systems of mating. Genetics. 1946;31:39-59.
6. Wright S. Isolation by distance. Genetics. 1943;28:114-38.
7. Malécot G. Les Mathématiques de l'Hérédité. Paris: Masson; 1948.
8. Malécot G. Heterozygosity and relationship in regularly subdivided populations. Theor Popul Biol. 1975;8:212-41.
9. Malécot G. Génétique des populations diploïdes naturelles dans le cas d'un seul locus. III. Parenté, mutations et migration. Ann Génét Sél Anim. 1973;5(3):333-61.
10. Vekemans X, Hardy OJ. New insights from fine-scale spatial genetic structure analyses in plant populations. Mol Ecol. 2004;13(4):921-35. doi: 10.1046/j.1365-294X.2004.02076.x.
11. Meirmans PG. The trouble with isolation by distance. Mol Ecol. 2012;21(12):2839-46. doi: 10.1111/j.1365-294X.2012.05578.x.
12. Koenig WD, Van Vuren D, Hooge PN. Detectability, philopatry, and the distribution of dispersal distances in vertebrates. Trends Ecol Evol. 1996;11(12):514-7.
13. Broquet T, Petit EJ. Molecular estimation of dispersal for ecology and population genetics. Annu Rev Ecol, Evol Syst. 2009;40(1):193-216. doi: 10.1146/annurev.ecolsys.110308.120324.
14. Epperson BK. Estimating dispersal from short distance spatial autocorrelation. Heredity (Edinb). 2005;95(1):7-15. doi: 10.1038/sj.hdy.6800680. PMID: 15931252.
15. Rousset F. Genetic differentiation and estimation of gene flow from F-statistics under isolation by distance. Genetics. 1997;145:1219-28.
16. Li MH, Merila J. Genetic evidence for male-biased dispersal in the Siberian jay (Perisoreus infaustus) based on autosomal and Z-chromosomal markers. Mol Ecol. 2010;19(23):5281-95. doi: 10.1111/j.1365-294X.2010.04870.x. PMID: 20977509.
17. Slatkin M. Gene flow in natural populations. Annu Rev Ecol Syst. 1985;16:393-430.
18. Excoffier L, Foll M, Petit RJ. Genetic consequences of range expansions. Annu Rev Ecol, Evol Syst. 2009;40(1):481-501. doi: 10.1146/annurev.ecolsys.39.110707.173414.
19. Leighton GM, Echeverri S. Population genomics of Sociable Weavers *Philetairus socius* reveals considerable admixture among colonies. Journal of Ornithology. 2016;157:483-92. doi: 10.1007/s10336-015-1307-1.

20. Garroway CJ, Radersma R, Sepil I, Santure AW, De Cauwer I, Slate J, et al. Fine-scale genetic structure in a wild bird population: the role of limited dispersal and environmentally based selection as causal factors. Evolution. 2013;67(12):3488-500. doi: 10.1111/evo.12121. PMID: 24299402.

21. Temple HJ, Hoffman JI, Amos W. Dispersal, philopatry and intergroup relatedness: fine-scale genetic structure in the white-breasted thrasher, *Ramphocinclus brachyurus*. Mol Ecol. 2006;15(11):3449-58. doi: 10.1111/j.1365-294X.2006.03006.x. PMID: 16968282.

22. Foerster K, Valcu M, Johnsen A, Kempenaers B. A spatial genetic structure and effects of relatedness on mate choice in a wild bird population. Mol Ecol. 2006;15(14):4555-67. doi: 10.1111/j.1365-294X.2006.03091.x. PMID: 17107482.

23. Quaglietta L, Fonseca VC, Hájková P, Mira A, Boitani L. Fine-scale population genetic structure and short-range sex-biased dispersal in a solitary carnivore, *Lutra lutra*. J Mammal. 2013;94(3):561-71. doi: 10.1644/12-mamm-a-171.1.

24. Weber JN, Bradburd GS, Stuart YE, Stutz WE, Bolnick DI. Partitioning the effects of isolation by distance, environment, and physical barriers on genomic divergence between parapatric threespine stickleback. Evolution. 2016. doi: 10.1111/evo.13110. PMID: 27804120.

25. van Dijk RE, Covas R, Doutrelant C, Spottiswoode CN, Hatchwell BJ. Fine-scale genetic structure reflects sex-specific dispersal strategies in a population of sociable weavers (*Philetairus socius*). Mol Ecol. 2015;24(16):4296-311. doi: 10.1111/mec.13308. PMID: 26172866.

26. Dobson FS. Competition for mates and predominant juvenile male dispersal in mammals. Anim Behav. 1982;30:1183-92.

27. Greenwood PJ. Mating systems, philopatry and dispersal in birds and mammals. Anim Behav. 1980;28:1140-62.

28. Goudet J, Perrin N, Waser P. Tests for sex-biased dispersal using bi-parentally inherited genetic markers. Mol Ecol. 2002;11:1103-14.

29. Roy J, Gray M, Stoinski T, Robbins MM, Vigilant L. Fine-scale genetic structure analyses suggest further male than female dispersal in mountain gorillas. BMC Ecol. 2014;14:21.

30. Prugnolle F, de Meeus T. Inferring sex-biased disperasl from population genetic tools: a review. Heredity. 2002;88:161-5. doi: 10.1038/sj/hdy/6800060.

31. Segurel L, Martinez-Cruz B, Quintana-Murci L, Balaresque P, Georges M, Hegay T, et al. Sex-specific genetic structure and social organization in Central Asia: insights from a multi-locus study. PLoS Genet. 2008;4(9):e1000200. doi: 10.1371/journal.pgen.1000200. PMID: 18818760.

32. Woolfenden GE, Fitzpatrick JW. The Florida Scrub Jay: Demography of a Cooperative-breeding Bird. Princeton, New Jersey: Princeton University Press; 1984.

33. Woolfenden GE, Fitzpatrick JW. Florida Scrub-Jay (*Aphelocoma coerulescens*). Poole A, editor. Ithaca: Cornell Lab of Ornithology; 1996.

34. Fitzpatrick JW, Woolfenden GE, Bowman R. Dispersal distance and its demographic consequences in the Florida Scrub-Jay. In: Adams NJ, Slotow RH, editors. Proceedings of the XXII International Ornithological Congress; 1999; Durban: South Africa. pp. 2465-2479.

598 35. Schoech SJ, Mumme RL, Moore MC. Reproductive endocrinology and mechanisms of breeding inhibition in cooperatively breeding Florida Scrub Jays
600 (*Aphelocoma c. coerulescens*). Condor. 1991;93:354-64.
36. Chen N, Cosgrove Elissa J, Bowman R, Fitzpatrick John W, Clark Andrew G.
602 Genomic consequences of population decline in the endangered Florida Scrub-Jay. Curr Biol. 2016. doi: 10.1016/j.cub.2016.08.062.
604 37. Schaffner SF. The X chromosome in population genetics. Nat Rev Genet. 2004;5(1):43-51. doi: 10.1038/nrg1247. PMID: 14708015.
606 38. Charlesworth B. Effective population size and patterns of molecular evolution and variation. Nat Rev Genet. 2009;10(3):195-205. doi: 10.1038/nrg2526. PMID: 19204717.
608 39. Ishida Y. Sewall Wright and Gustave Malécot on isolation by distance. Philosophy of Science. 2009;76(5):784-96.
610 40. Slatkin M, Veuille M. Modern developments in theoretical population genetics: the legacy of Gustave Malécot: Oxford University Press; 2002.
612 41. Nagylaki T. Gustave Malécot and the transition from classical to modern population genetics. Genetics. 1989;122(2):253-68.
614 42. Ralph P, Coop G. The geography of recent genetic ancestry across Europe. PLoS Biol. 2013;11(5):e1001555. doi: 10.1371/journal.pbio.1001555. PMID: 23667324.
616 43. Ringbauer H, Coop G, Barton NH. Inferring recent demography from isolation by distance of long shared sequence blocks. bioRxiv. 2016. doi: 10.1101/076810.
618 44. Baharian S, Barakatt M, Gignoux CR, Shringarpure S, Errington J, Blot WJ, et al. The Great Migration and African-American Genomic Diversity. PLoS Genet.
620 2016;12(5):e1006059. doi: 10.1371/journal.pgen.1006059.
45. Browning SR, Browning BL. Identity by descent between distant relatives:
622 detection and applications. Annu Rev Genet. 2012;46:617-33. doi: 10.1146/annurev-genet-110711-155534. PMID: 22994355.
624 46. Mumme RL. Do helpers increase reproductive success? Behav Ecol Sociobiol. 1992;31:319-28.
626 47. ESRI. ArcGIS Desktop: Release 10. Redlands, CA: Environmental Systems Research Institute; 2011.
628 48. Greenwood PJ, Harvey PH. The natal and breeding dispersal of birds. Annu Rev Ecol Syst. 1982;13:1-21. doi: 10.1146/annurev.es.13.110182.000245.
630 49. Purcell S, Neale B, Todd-Brown K, Thomas L, Ferreira M, Bender D, et al. PLINK: a toolset for whole-genome association and population-based linkage analysis.
632 Am J Hum Genet. 2007;81:559-75.
50. Therneau TM, Sinnwell J. kinship2: Pedigree Functions. 2015.
634 51. R Core Team. R: A language and environment for statistical computing. Vienna, Austria: R Foundation for Statistical Computing; 2015.
636 52. Kardos M, Luikart G, Allendorf FW. Measuring individual inbreeding in the age of genomics: marker-based measures are better than pedigrees. Heredity (Edinb).
638 2015;115(1):63-72. doi: 10.1038/hdy.2015.17. PMID: 26059970.
53. Oksanen J, Blanchet FG, Kindt R, Legendre P, Minchin PR, O'Hara RB, et al.
640 vegan: Community Ecology Package. 2015.
54. Mantel N. The detection of disease clustering and a generalized regression
642 approach. Cancer Res. 1967;27:209-20.

55. Mantel N, Valand RS. A technique of nonparametric multivariate analysis. Biometrics. 1970;26(3):547-58.

56. Grossman M, Eisen EJ. Inbreeding, coancestry, and covariance between relatives for X-chromosome loci. J Hered. 1989;80:137-42.

Figures

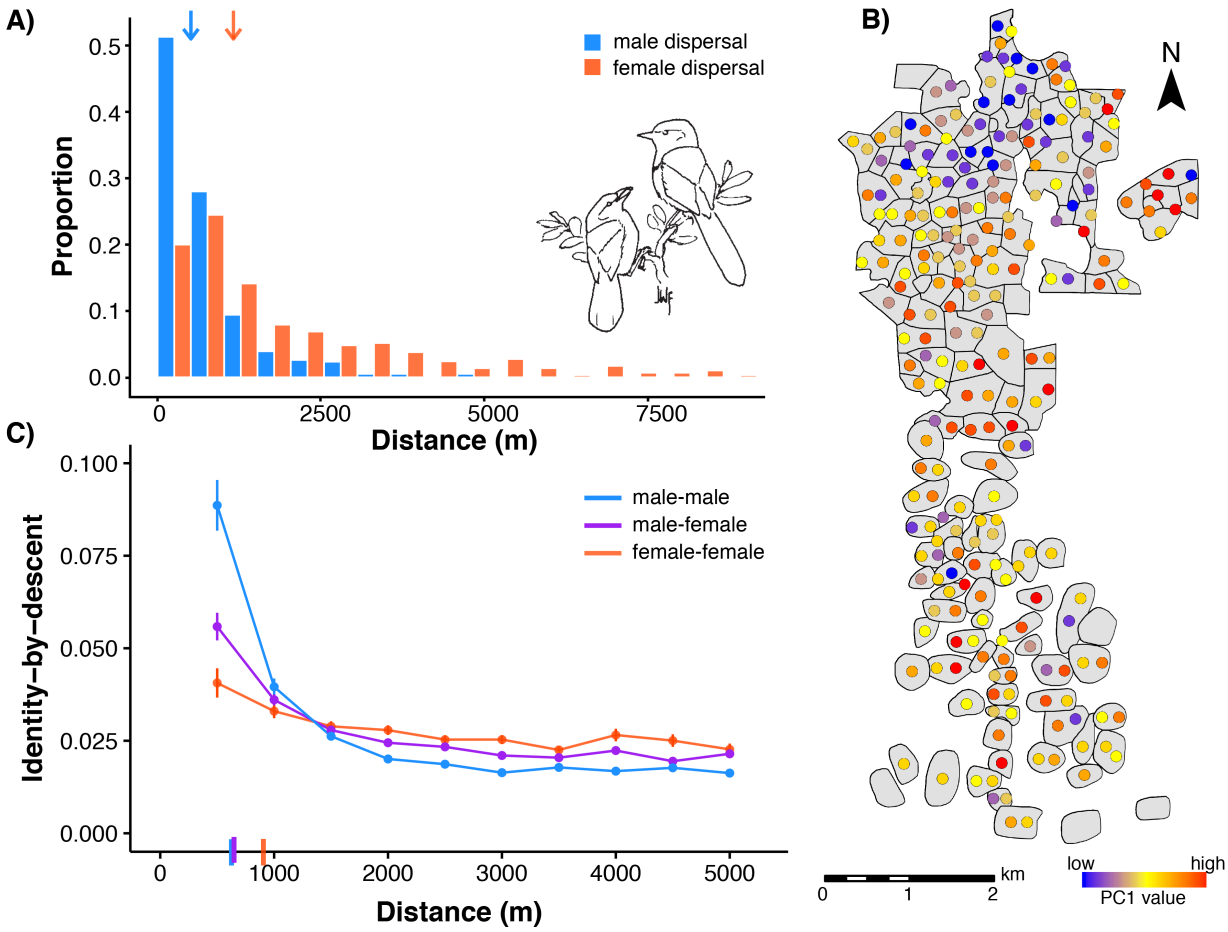

Fig 1. Dispersal curves and isolation-by-distance patterns in the Florida Scrub-Jay

(A) Natal dispersal distances for Florida Scrub-Jays born and breeding within Archbold Biological Station (1990-2013, *n* = 672) are significantly shorter in males (blue bars; median ± SE = 488 ± 43 m) than in females (salmon bars; 1149 ± 108 m; Wilcoxon rank sum test: $p = 2.2 \times 10^{-16}$). Median values are shown with arrows at top of plot. Florida Scrub-Jay drawing by JWF. **(B)** Map of breeding territories (gray polygons) for a representative year (2008) within Archbold with individual breeders colored by PC1 values shows isolation-by-distance from north to south. **(C)** Isolation-by-distance

patterns in autosomal SNPs shown with standard error bars. The decline in IBD with
660 geographic distance is stronger in male-male (blue) and male-female (purple) pairwise comparisons than in female-female comparisons (salmon). δ values, the distance where
662 IBD drops halfway to the mean (see text for details), are shown as dashes on the x-axis.

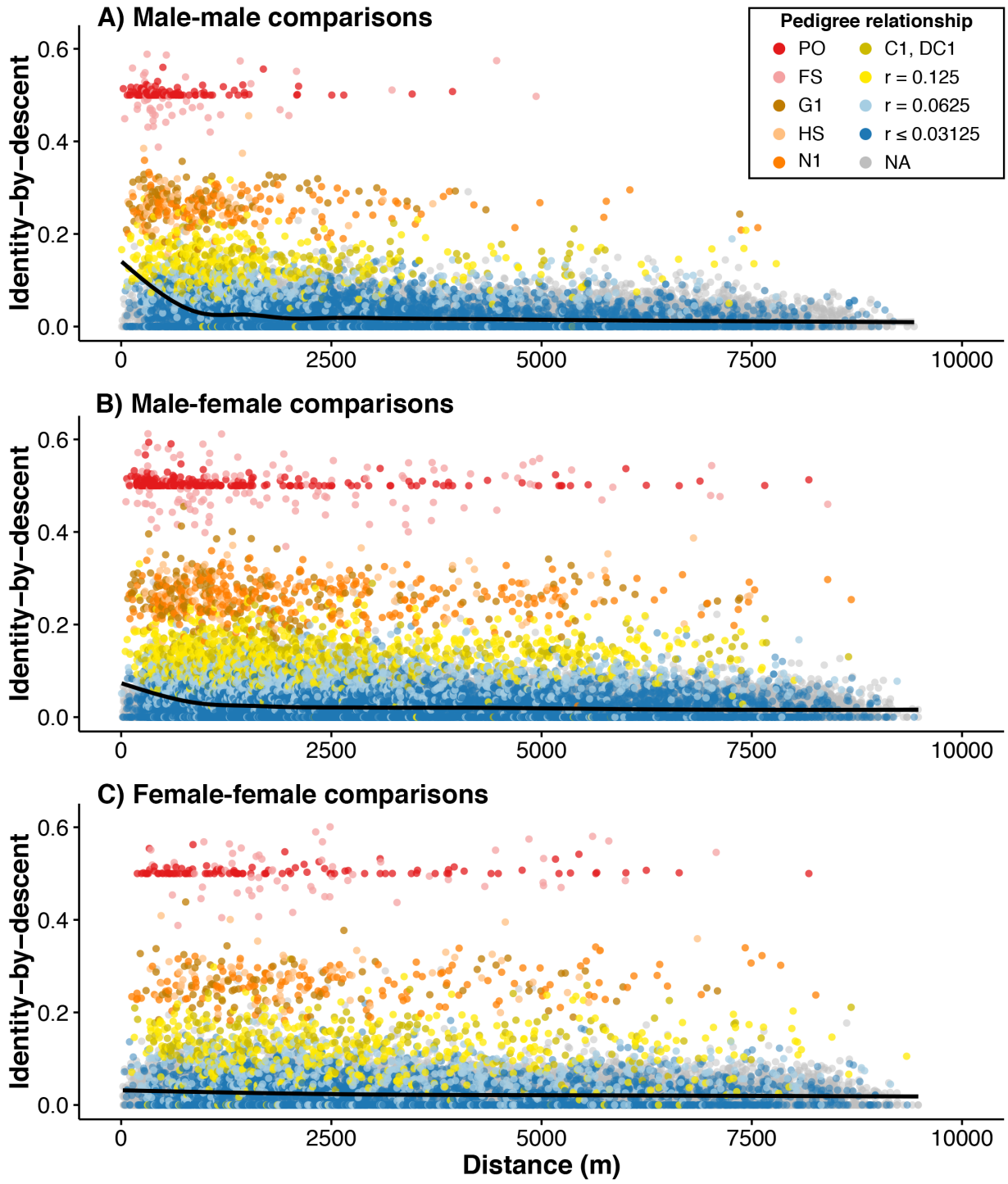

664

Fig 2. Isolation-by-distance patterns in Florida Scrub-Jays can be deconstructed

666 **by pedigree relatedness**

Distance versus IBD in autosomal SNPs for all possible **(A)** male-male, **(B)** male-female, and **(C)** female-female comparisons is, in part, generated by highly related individuals remaining physically close together. Loess curves are shown in each panel. Isolation-by-distance patterns are significantly stronger in male-male (A) and male-female (B) comparisons than in female-female (C) comparisons. Points are colored by specific pedigree relationship or, for more distant relationships, grouped into a single coefficient of relationship (*r*) class. Gray points indicate no known pedigree relationship. Pedigree relationship abbreviations: PO = parent-offspring, FS = full-siblings, G1 = grandparent-grandchild, HS = half-siblings, N1 = aunt/uncle-nibling, C1 = first cousins, DC1 = double first cousins. (“Nibling” is a gender-neutral term for niece and nephew.)

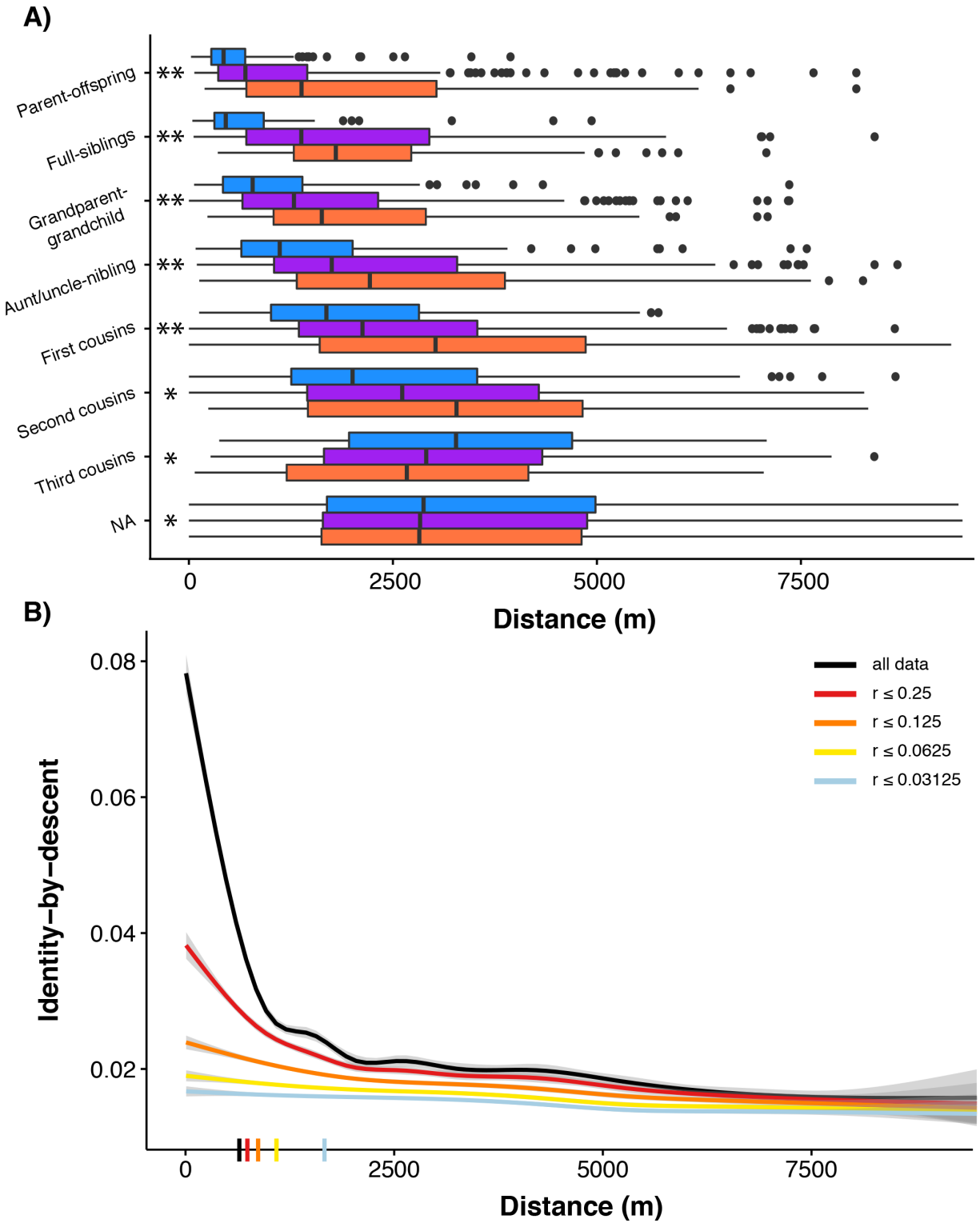

678

Fig 3. Distances between Florida Scrub-Jay individuals of close pedigree

680 **relatedness explains, in part, the isolation-by-distance patterns**

(A) Distances between all possible male-male (blue), male-female (purple), and female-female (salmon) comparisons separated by pedigree relationship. Significant differences using the Kolmogorov-Smirnov Test are indicated with two asterisks when all three comparisons were significantly different (MM-FF, MM-MF, MF-FF) and a single asterisk when only MM-FF and MM-MF comparisons were significantly different. The distance between parent-offspring pairs is significantly shorter than the distance between full-siblings (Wilcoxon rank sum test, $p = 5.20 \times 10^{-9}$) and the distance between full-siblings is significantly shorter than the distance between pairs with $r = 0.25$ (Wilcoxon rank sum test, $p = 0.01$). **(B)** Loess curves of distance versus IBD in autosomal SNPs for all possible unique pairwise comparisons with separate lines showing sequential removal of pedigree relationship classes. The strength of isolation-by-distance decreases as highly related pairs are removed. δ values, the distance where IBD drops halfway to the mean (see text for details), are shown as dashes on the x-axis.

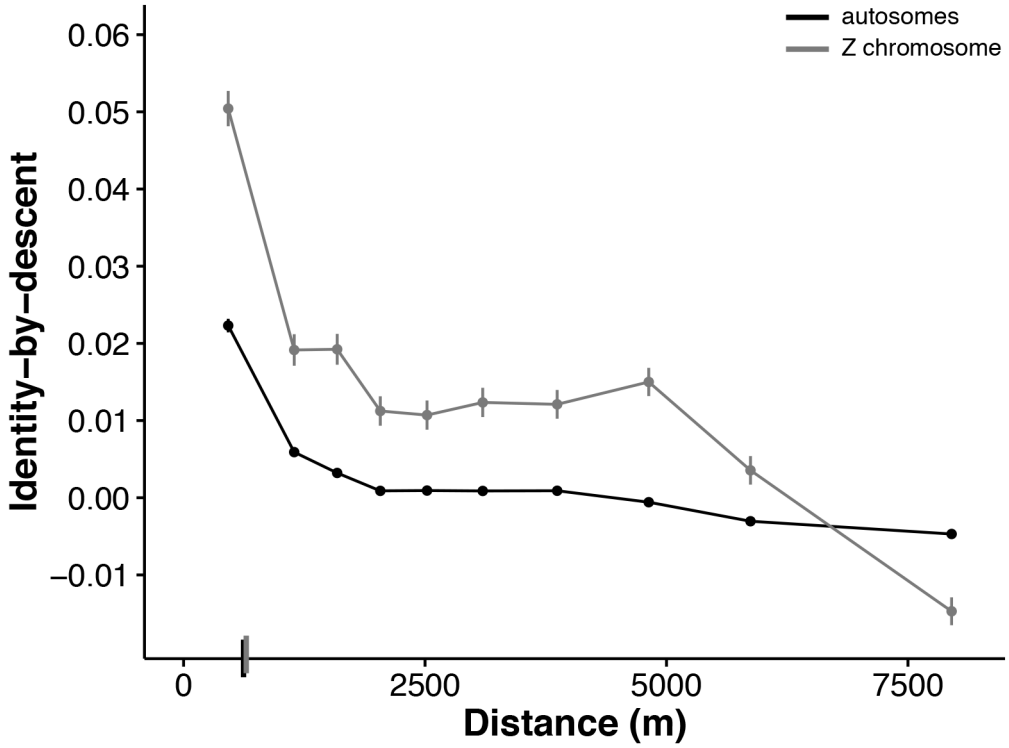

696

Fig 4. Isolation-by-distance in autosomal and Z-linked SNPs

698 Geographic distance versus unbiased IBD for autosomal (black) and Z-linked (gray) SNPs for all possible unique pairwise comparisons showing higher mean IBD in Z-

700 linked SNPs (0.014) than in autosomal SNPs (0.0027). IBD values are binned across 10 distance quantiles and shown as mean ± SE. δ values, the distance where IBD drops

702 halfway to the mean (see text for details), are shown as dashes on the x-axis.

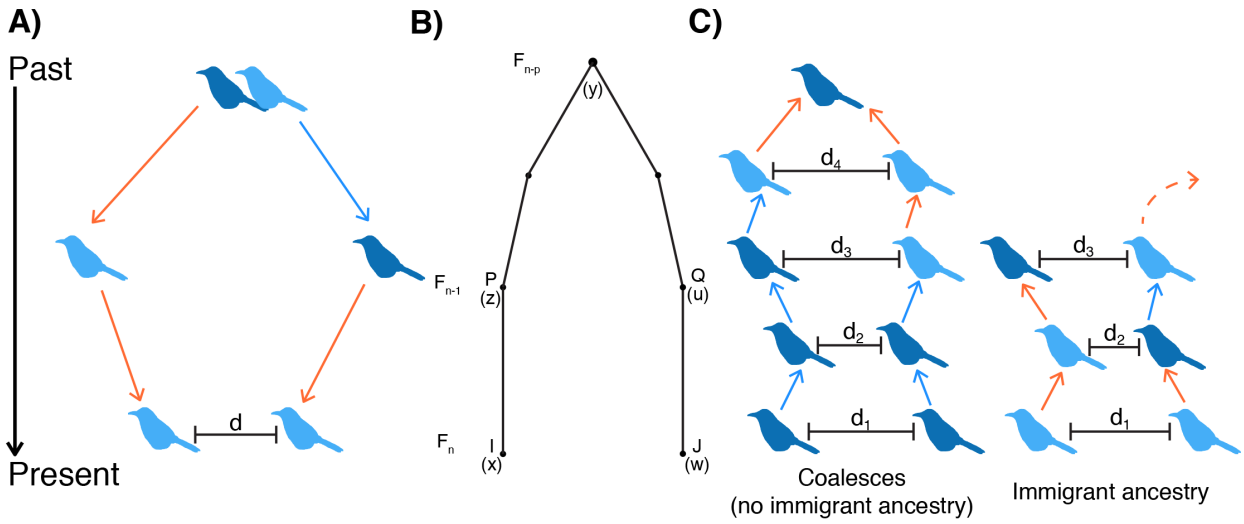

Fig 5. Overview of dispersal and coalescent simulations of isolation-by-distance

(A) An example schematic of a dispersal simulation for two female first cousins. Our simulations were over a two-dimensional space, but here we show dispersal on a one-dimensional line for visualization purposes. For the dispersal simulations, we start with the most recent common ancestor for a pair of individuals of known pedigree relationship and simulate dispersal events forward in time until the present. In this case, we start at the grandparental nest, simulate dispersal distances (and angles) of the parents, and then dispersal of the two cousins. Light blue birds are females and dark blue are males. Arrows indicate male (blue) and female (salmon) dispersal drawn from the dispersal curves. Sexes of all ancestors are determined by a coin flip. **(B)** The gametic kinship chain from Malécot's theory of isolation-by-distance. A locus from individual *I* born at location *x* and a locus from individual *J* born at location *w* in generation F_n are IBD if both are descended from the same locus in their common ancestor in generation F_{n-p}. Under Malécot's model, genetic relatedness of individuals should decrease as the distance between them increases. Redrawn from [9]. **(C)** Illustration of two possible outcomes in the coalescent simulations. In these simulations,

we start with a pair of individuals of specified sex separated by distance d_1 and trace their ancestral lineages backwards in time until we either reach a common ancestor or one of the ancestors was an immigrant. In each generation, the probability a given pair coalesces is sampled directly from the pedigree. M is the probability a parental individual is an immigrant. Using empirical estimates of IBD between closely related pairs and immigrants, we generated expected IBD values for each pair.

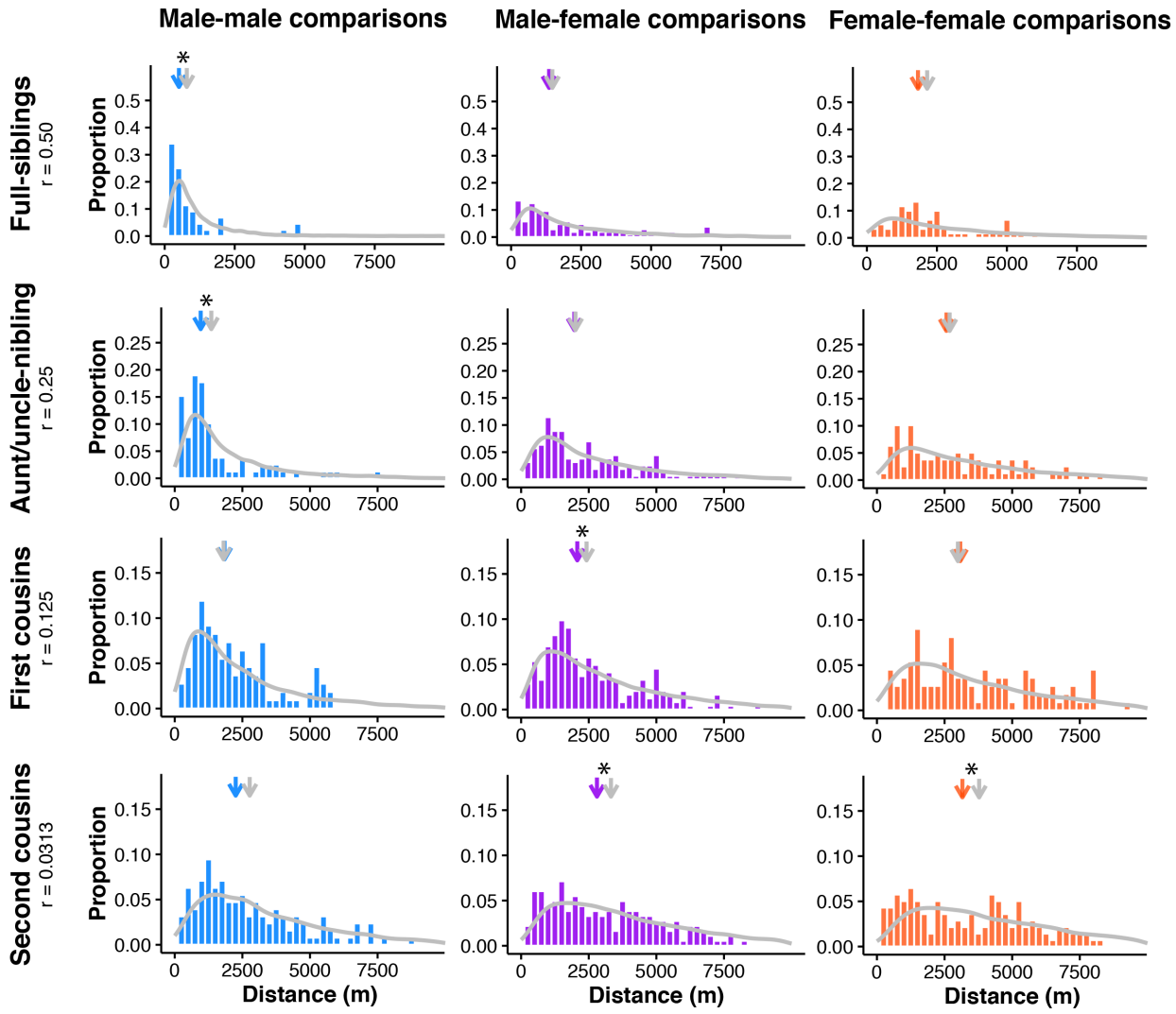

728

Fig 6. Dispersal simulations can reconstruct the observed distribution of

730 **geographic distances between related pairs**

Simulated (gray line) and observed (colored histograms) dispersal values for full-

732 siblings, aunt/uncle-nibling, first cousin, and second cousin comparisons. Male-male comparisons are shown in blue, male-female comparisons in purple, and female-female

734 comparisons in salmon. Median values for the simulated (gray) and observed (colored) distributions are indicated by arrows above each plot. Simulated distributions that were

736 significantly different from the observed distribution using the Kolmogorov-Smirnov Test are marked with asterisks above the median arrows.

738

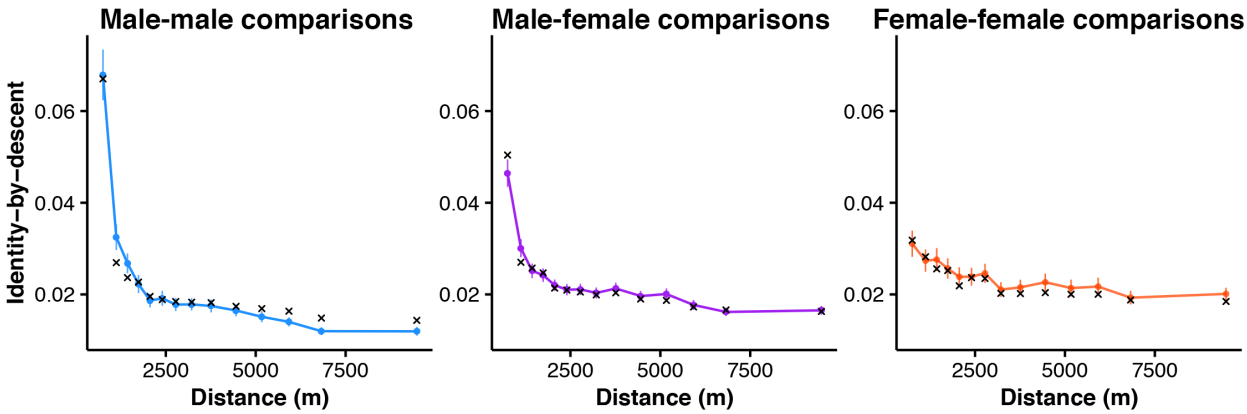

740

Fig 7. Coalescent simulations can reconstruct isolation-by-distance patterns

742 Simulated (black crosses) autosomal isolation-by-distance patterns for male-male (blue), male-female (purple), and female-female comparisons (salmon) using the

744 observed pedigree, dispersal curves, and immigration rate can recover the observed (colored circles and line) pattern of isolation-by-distance. The coefficient of

746 determination is 0.98 for male-male comparisons, 0.96 for male-female comparisons, and 0.78 for female-female comparisons.